

An investigation of moldability and mechanical properties of MgO added alumina

O. Erdem^{1*}, L. Urtekin¹, İ. Uslan²

¹*Department of Mechanical Engineering, Faculty of Engineering and Architecture, Ahi Evran University, Merkez/Kırşehir, Turkey*

²*Department of Mechanical Engineering, Faculty of Engineering, Gazi University, 06570 Ankara, Turkey*

Received 24 April 2017, received in revised form 5 August 2017, accepted 26 January 2018

Abstract

In this study, the influence of MgO addition on mechanical properties of the injection molded alumina was investigated. Firstly, alumina feedstocks (without adding MgO) were prepared to determine the optimum powder/binder ratio by the capillary rheometer. Then, MgO was added at 0.5, 1 and 1.5 wt.% to alumina feedstocks at the optimum ratio. Moldflow simulation analysis (MSA) was performed to obtain injection parameters (injection pressure, flow rate and feedstock temperature) before the real molding operation. Through the agency of the pre-operating parameters obtained from MSA, preliminary trials were carried out by molding machine for successful specimens (tensile and bending). By comparison of experimental and analytical results, the error rate of injection parameters was determined for both specimens. The maximum strengths of bending and tensile test values were found 158 MPa and 69 MPa (in specimens containing 1 wt.% MgO), respectively. Analysis of SEM revealed that specimens containing 1 wt.% MgO had less porosity.

Key words: alumina, powder injection molding, rheology, sintering, moldability

1. Introduction

Powder injection molding (PIM) is an impressive method for the mass production of complex and dimensionally accurate parts with metal and ceramic powders [1]. The process is the hybrid of powder technology and conventional plastic injection molding [2]. The PIM includes fundamentally four stages: powder-binder mixing, injection molding, debinding and sintering [2–7]. The powder is mixed with an ideal binder system to obtain a viscous flow to injection mold into the desired geometry. Injection molding stage involves the steps: melting and mixing of feedstock (powder-binder mixture), injecting the melted feedstock to mold cavity with the help of pressure, forming the melted feedstock into the desired shape, packing, cooling-solidification and finally, the ejection of the molded product [8]. During the molding cycle, there can occur some defects such as incomplete filling, oc-

ular discharge, warpage, flow mark and jetting mark due to wrong input parameters [9]. To reduce these problems occurring in molding cycle, several software products have been recently available in the market, for instance, Moldflow and Moldex3D. This software helps to analyze the flow characteristic of feedstocks. The outputs of analysis can be used as pre-operating parameters in injection molding [10]. After the successful molding process, the binder is eliminated from the molded part usually by debinding processes. The debinding is the most difficult stage due to the formation of defects, for example, swelling and cracking in the part body. To overcome or reduce these problems, different debinding techniques have been improved [1, 11–15]. In the final stage, the porous part is sintered to compact the desired properties [16].

In recent years, ceramic components are introduced in new fields of application, especially for high temperature and wear applications in which polymer

*Corresponding author: tel.: 386-286-38-25; e-mail address: oguz.erdem@ahievran.edu.tr

Table 1. Physical properties of binder system constituents

Material	Manufacturer	Density (g cm ⁻³)	Melting point (°C)
PEG8000	Alfa Aesar	1.204	62
PP	Petkim A.S.	0.85	189
SA	Merck Co.	0.94	69

or metal components are not suitable [17]. In these applications, alumina is of primary importance because of its high hardness, good corrosion resistance, high insulation and ease of processing characteristics [18]. Mechanical properties of alumina are directly proportional to its sintered density [19]. There are two sintering methods in use to obtain closer density than the theoretical density of alumina: the first method is pressure-less sintering with additives and the second method is pressure sintering such as hot isostatic pressing (HIP). Due to high investment costs and the difficulties of flexible mold design, HIP is not usually a preferable method. On the other hand, pressure-less sintering method does not require extra investment costs and also provides easy fabrication options for alumina parts. Therefore, pressure-less sintering is a more common method in the market [20].

Several experimental studies were published in the literature explaining the beneficial effect of additives in alumina, such as MgO, TiO₂, ZrO₂, SiO₂, Y₂O₃ and Li₂O₃ [21–23]. The goal of the additives is to control the densification, grain growth and morphology during sintering. The ability to control microstructure is of central importance in achieving the desired mechanical properties [24]. It was reported that the addition of a small amount of MgO to alumina causes grain boundary roughening and hence the transformation from abnormal grain growth to normal growth behavior. The MgO addition causes some grain interfaces to provoke roughness at the atomic size. The grains also become almost coaxial. The amounts of the abnormal large grains increase up to the grain growth looks like the normal growth. This situation is coherent with the decreasing surface free energy related to interface roughening [25]. The MgO addition results in the formation of alumina with coaxial morphology, promotes normal grain growth and increases the part density [26].

The study aims to improve the alumina's mechanical properties with the addition of MgO, and also an investigation of the moldability of MgO added alumina feedstock. PIM method was preferred for this purpose. Firstly, Moldflow simulation analysis (MSA) was performed to obtain injection parameters before the real molding operation. After the preliminary experiments were conducted by the agency of the results of MSA, optimum injection parameters were determined. Secondly, tensile and bending specimens were molded by PIM method. Afterwards, both the debind-

ing and sintering conditions were optimized. Finally, mechanical tests were carried out.

2. Material and methods

The 99.6 % purity fused alumina ALODUR WSK F500 (Treibacher Schleifmittel Inc.) with a particle size (d_{50}) of 3.37 μm was used as raw material in this study. The powder has a density of 3.96 g cm⁻³ and a molecular weight of 101.9 g mol⁻¹. Commercial MgO powder with an average particle size of 6.37 μm was used as sintering additive material in the experiments. The additive powder has a density of 3.58 g cm⁻³ and a molecular weight of 40.30 g mol⁻¹.

A three-component binder system was selected for the work. The binder is the mixture of polyethylene glycol (PEG8000), polypropylene (PP) and stearic acid (SA) with a weight ratio of PEG8000/PP/SA = 65/30/5. PP acted as a backbone to give strength to green part up to the sintering process. PEG8000 was used as the major binder of a system for improving flowability. SA was used as a surfactant for the alumina and polymeric ingredients. The binder constituents and their properties are listed in Table 1.

The composition of the feedstock has great importance in PIM since it is to provide high green densities for sintering [27, 28]. A feedstock, which has good homogeneity, high stability, low viscosity at the processing temperature, proper flow behavior and low shear stress, enables the perfect injection molding [29]. Rheology experiments were carried out by capillary rheometer for fear that the clogging problem might occur in injection molding operation. So, four different feedstock formulations (Table 2) were prepared to obtain the optimum powder/binder ratio (critical powder loading). As the binder, 65 wt.% PEG8000, 30 wt.% PP and 5 wt.% SA mixture was used. Ten minutes were allowed to reach thermal equilibrium after charging the barrel. A 2 mm diameter and 8 mm length die was used for compaction. The rheologies of the feedstocks were studied using the ASTM D1238 and TS 1675 standard procedure within the temperature range of 170–210 °C and shear stress of 18.7 kPa.

Having evaluated rheological results, it was decided to the most appropriate feedstock formulation for the PIM. After then, theoretical density and other properties of this feedstock formulation were defined

Table 2. Some properties of feedstocks

Feedstock name	Formulation of feedstock (vol.%)	Theoretical density (g cm^{-3})
F1	51 alumina + 49 binder	2.553
F2	53 alumina + 47 binder	2.611
F3	56 alumina + 44 binder	2.7
F4	59 alumina + 41 binder	2.784

Table 3. The specimens dimension of molded tensile and bending part

Specimen type	Symbol	Dimension	
		Large (mm)	Small (mm)
Tensile	m	93.6	85.3
	$D1$	24.5	22.75
	$D2$	7.88	5.85
	$D3$	5.85	3.82
Bending	x	12.2	
	t	7.7	
	y	89.5	

in the Moldflow software, and three critical parameters (injection pressure, injection temperature and the feedstock flow rate) were detected. For tensile and bending specimens, Moldflow pre-operation parameters (MPP) were obtained by simulation analysis in separate molds. Designing of mold cavity tolerances and the calculation of dimensional shrinkage, the values determined by the Metal Powder Industry Federation were used [30]. The filling simulation of the specimens was carried out, and then, the obtained MPP gave an idea to preliminary experiments of the next step: injection molding. Afterwards, Moldflow Simulation Model (MSM) was verified with the help of experimental PIM operation parameters (POP).

Feedstocks were mixed as dry with a mixer (Turbula 3-Dimensional Shaker/Mixer) for 100 min. After the mixing process, feedstocks were extruded by a conical twin screw extruder (Kraus-Maffei). The rotational speed of the screw was set to 50 rpm, while the temperature of the barrel was maintained at 165 °C. The cylindrically extruded pellets with 3 mm diameter and 3–5 mm length were collected for injection molding. Tensile specimens and three-point bending specimens were molded by Arburg Allrounder 220S injection molding machine (Fig. 1). The specimens' dimensions of molded tensile and bending part are shown in Table 3.

A three-component binder system including both water-soluble (PEG8000) and insoluble (PP and SA) materials was removed with a solvent and thermal (pre-sintering) debinding process in this study. The solvent debinding was performed by immersing the specimens into the water at different temperatures

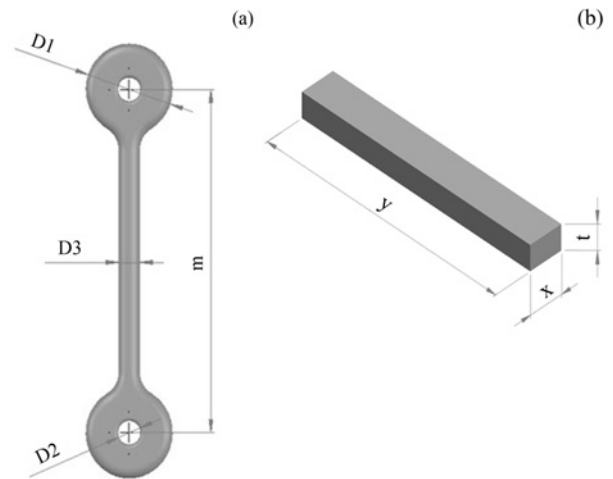


Fig. 1. The green test specimens: (a) tensile and (b) bending.

(35–65 °C). The PEG8000 was removed by solvent debinding process. The water-insoluble PP and SA materials were decomposed by thermal debinding. The sintering process was carried out in the air in a furnace (Carbolite, UK). Before the sintering process, the most suitable sintering parameters of the used alumina powder were determined by the tensile tests of sintered specimens containing 1 wt.% MgO.

Densities of the sintered specimens were calculated based on Archimedes principle. All the specimens surfaces were coated with a thin film by dipping into 5 wt.% paraffin wax in 95 wt.% xylene (TS 2305 and TS EN 623-2) solution. Volumetric shrinkage values were

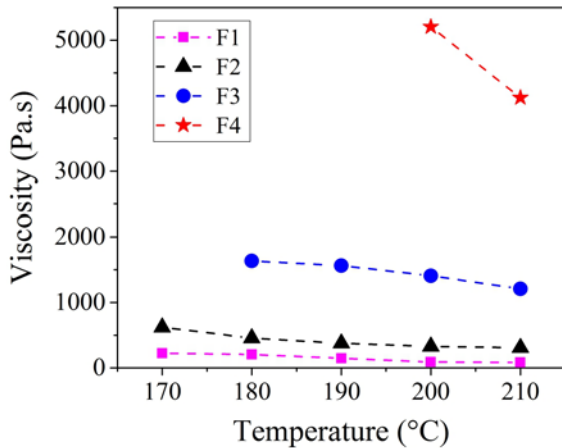


Fig. 2. The variation of viscosity vs. temperature for different feedstocks at 18.7 kPa shear stress.

found by measuring the specimen dimensions before and after the sintering process. Mechanical properties of the sintered specimens were obtained by tensile and three-point bending tests. Tensile (TS ISO 15490) and bending (TS ENV 12789) tests were performed using Shimadzu tensile testing machine of 5 kN capacity. Microstructure examinations were carried out using JEOL JSM-6060LV scanning electron microscopy (SEM).

3. Results and discussion

3.1. Results of Capillary Rheometer

Different feedstocks (F1, F2, F3 and F4) were examined under 18.7 kPa shear stress value at 170–210°C temperatures. The viscosity against temperature and shear rate variations was plotted for observing its suitability for PIM (Figs. 2 and 3). The rheological properties of F1 seem to be appropriate for PIM at first glance according to the rheology analyses. However, the shear rate values of F1 are higher than the other feedstocks shear rate values which may cause separation of powder/binder under the high injection pressure. Moreover, to obtain full density part by PIM, the solid loading rate of the feedstock must reach its maximum value.

Feedstock F3 exhibited poor flowability at 170°C, and its viscosity values were quite high at the higher temperature values. So, the critical loading value of the mixture (alumina-binder) is decided as 56 vol.% alumina powder. To avoid the wear of the mixing and molding equipment, the optimal solid loading which is approximately 2 to 5 vol.% lower than critical loading value was used. Also, during injection molding shear rates vary between 100 and 1000 s⁻¹ and the flow during molding requires a viscosity less than 1000

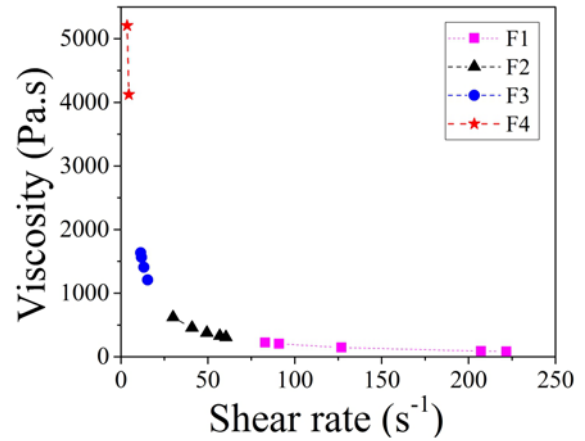


Fig. 3. The variation of viscosity vs. shear rate for different feedstocks at 18.7 kPa shear stress.

Pa s⁻¹ [31]. Hence, the optimum powder/binder ratio was chosen as 53/47 vol.% (F2).

F2 showed the most proper pseudo-plastic behavior. The viscosities of F2 are under 1000 Pa s⁻¹ at all tested temperatures. The shear rates of F2 are smaller than 100 s⁻¹ for 18.7 kPa shear stress. It has been foreseen that the addition of MgO does not change the rheological properties of alumina since the density values of alumina and MgO are close to each other. Four different feedstocks (for pure alumina feedstock and 0.5, 1, 1.5 wt.% MgO added alumina feedstocks) with F2 formulation were prepared for examining the rheological properties. The variation of viscosity against temperature and the shear rate were obtained for deciding its suitability for PIM (Figs. 4 and 5). In Figs. 4 and 5, the viscosities of all feedstocks under 1000 Pa s⁻¹ for the measured temperatures are shown. The shear rates of them are smaller than 100 s⁻¹. Over and above, the curves of feedstocks, which indicate the same rheological behavior, have almost overlapped (Fig. 5). All feedstocks showed a pseudo-plastic flow behavior suitable for PIM.

3.2. The results of Moldflow Simulation Analysis (MSA)

The molding parameters (feedstock temperature, pressure and melt flow index values) were determined by capillary rheometer studies, and they were also used in MSM designing. As a result of the rheology experiments, it had already been determined that the F2 feedstock was the most suitable feedstock for the PIM. So, the rheological properties (viscosity, shear rate, pressure, temperature, etc.) and physical properties (theoretical density, etc.) of the F2 feedstock were defined in the MSM. The filling analysis of the F2 feedstock was carried out by the solid models which were prepared according

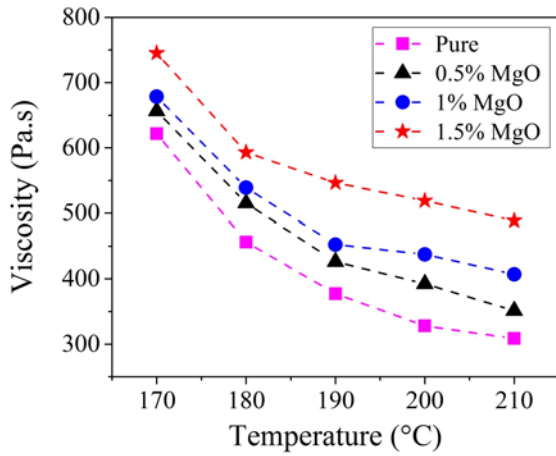


Fig. 4. The variation of viscosity vs. temperature for MgO added feedstocks with F2 formulation at 18.7 kPa shear stress.

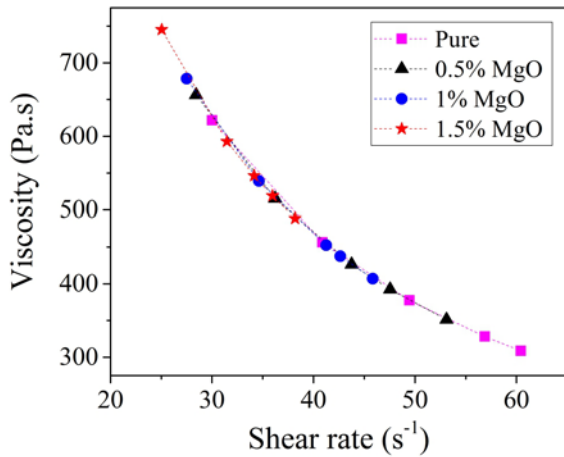


Fig. 5. The variation of viscosity vs. shear rate for MgO added feedstocks with F2 formulation at 18.7 kPa shear stress.

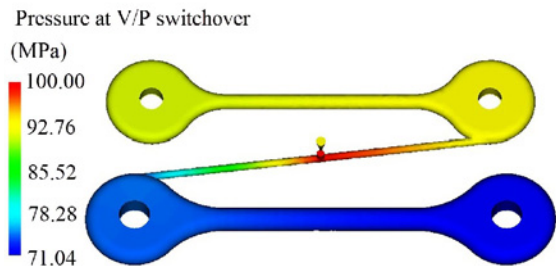


Fig. 6. The injection pressure of tensile specimens during the molding simulation.

to the dimensions of the tensile and bending specimens.

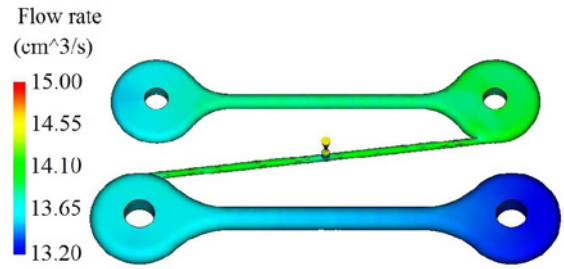


Fig. 7. The flow rate of tensile specimens during the molding simulation.

Figure 6 shows the distribution of injection pressures during the molding simulation of tensile specimens. At first glance, it is seen that the pressure values are high in the runner parts and at the first entry point of mold. It is scientifically expected that injection pressure should be high in places where the mold cross-section is narrowed. By the same token, the regions where the mold cross-section expands, pressure decreases are observed due to the drop in feedstock flow. In particular, it can be seen that the pressure value of large tensile specimen is lower than that of the small one. This is because the large tensile specimen's cross-section area is larger than that of the small one. A maximum pressure value of 92.76 MPa is observed from a small tensile specimen on the side of the mold, while a minimum pressure value of 71.07 MPa is detected on the large tensile specimen side. The average pressure value is calculated as 81.9 MPa for tensile specimens with pressure values in the range of 71.04–92.76 MPa. This pressure value is used for the first trial during the molding operation.

During the molding simulation, the flow rate values of tensile specimens showed changes concerning cross-sectional area, similar to injection pressure values (Fig. 7). That is, the flow rate is inversely proportional to the cross-sectional area. As can be seen in Fig. 7, especially, the flow rate has decreased to 13.20 cm³ s⁻¹ at the tip of the large tensile specimen. For this region, it is thought that incomplete filling might occur and it might be difficult to reach full density. Therefore, to avoid these problems, it has been decided that the flow rate value should be increased during the real injection of the operation. The average flow rate value is calculated as 13.8 cm³ s⁻¹ for tensile specimens with flow rate values in the range of 13.2–14.55 cm³ s⁻¹. So, 13.8 cm³ s⁻¹ flow rate value has been tried as an input parameter during the molding stage.

In injection molding machines, the feedstock temperature is controlled by spiral heating resistances and thermocouples in the barrel. By the time the feedstock comes to the injection nozzle, it is heated in echelon and consistently mixed by twin screws in the bar-

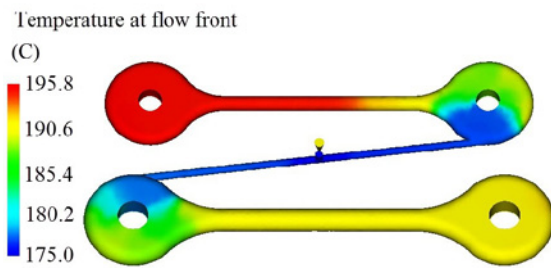


Fig. 8. The injection temperature of tensile specimens during the molding simulation.

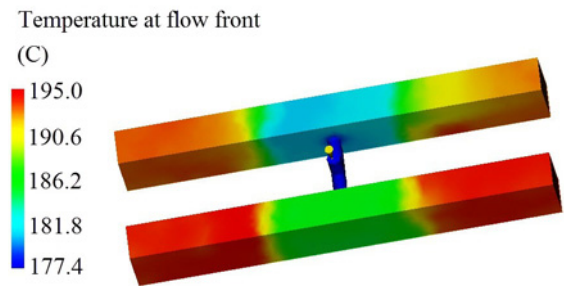


Fig. 11. The injection temperature of bending specimens during the molding process.

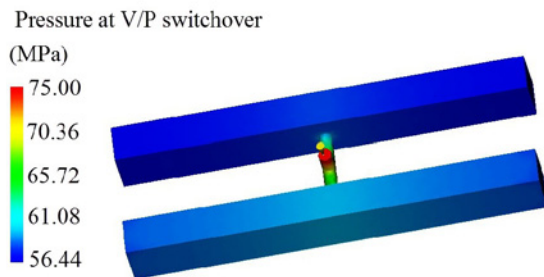


Fig. 9. The injection pressure of bending specimens during the molding process.

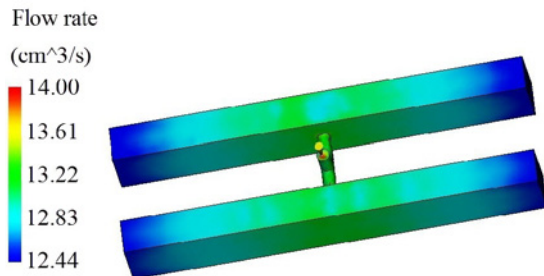


Fig. 10. The flow rate of bending specimens during the molding process.

rel. Thus, feedstock temperature is accepted to be the temperature value at the end of the injection nozzle. In analyses performed for both tensile and bending specimens, the mold surface temperature is defined as 20°C and the feedstock temperature as 200°C . In Fig. 8, it is also thought that the melted feedstock waited for a relatively short time on the mold runners. For this reason, these zones have lower temperature values in the analysis. This situation is true for the actual molding process as well. As it can be seen on the small tensile specimen side of the mold, the reason for the high-temperature value is that melted feedstock can reach this region faster and stay for a relatively long time.

The pressure distribution of bending specimens is given in Fig. 9. Comments were made for the ten-

sile specimens and are similarly valid for the bending specimens. The pressure values are high at the runners and the entrance section of the mold, whereas the pressure values are relatively low at the specimens portion of the mold because of enlargement of the cross-sectional area. The average pressure value is calculated as 58.7 MPa for bending specimens with pressure values in the range of $56.44\text{--}61.08\text{ MPa}$. Hence, 58.7 MPa pressure value has been tried as a pre-operation parameter.

When it comes to the bending specimens' flow rate analysis, similar to pressure distribution results of bending specimens, it is detected that the flow rate is inversely proportional to the cross-sectional area (Fig. 10). It has been suspected that collapse may occur owing to reduced flow rates at the surface regions of bending specimens. The average flow rate value was calculated as $12.8\text{ cm}^3\text{ s}^{-1}$ for bending specimens with flow rate values in the range of $12.44\text{--}13.22\text{ cm}^3\text{ s}^{-1}$. As a result, $12.8\text{ cm}^3\text{ s}^{-1}$ flow rate value has been tried as an input parameter for the injection molding. Also, as can be understood in Fig. 11, the melted feedstock rapidly passes through the runners and fills the mold quickly. On account of the fact that feedstock flowed through the mold runners fast, the temperature distribution in these regions is relatively low.

3.3. Injection molding and validation of Moldflow Simulation Model (MSM)

In molding cycle, previously prepared feedstocks having the form of granules were used. Tensile and bending specimens were molded using four different feedstocks (for pure alumina feedstock and 0.5, 1, 1.5 wt.% MgO added alumina feedstocks) with the F2 formulation.

The pre-operation parameters obtained from the Moldflow analysis (Table 4) have been tested in the injection molding process. Injection pressure value of 81.9 MPa was tried as a pre-operation parameter in the molding of tensile specimens, but this input parameter occurred defect such as incomplete filling

Table 4. The average Moldflow Pre-operation Parameters (MPP)

Specimen	Average molding pressure (MPa)	Average feedstock flow rate ($\text{cm}^3 \text{s}^{-1}$)	Average feedstock temperature ($^{\circ}\text{C}$)
Tensile	81.9	13.8	200
Bending	58.7	12.8	200

Table 5. The most suitable PIM Operation Parameters (POP)

Specimen	Molding pressure (MPa)	The amount of getting feedstock (cm^3)	Feedstock flow rate ($\text{cm}^3 \text{s}^{-1}$)	Barrel temperature ($^{\circ}\text{C}$)	Feedstock temperature ($^{\circ}\text{C}$)
Tensile	115	16	17	35-185-195-205-215	215
Bending	95	15	17	35-185-195-205-215	215

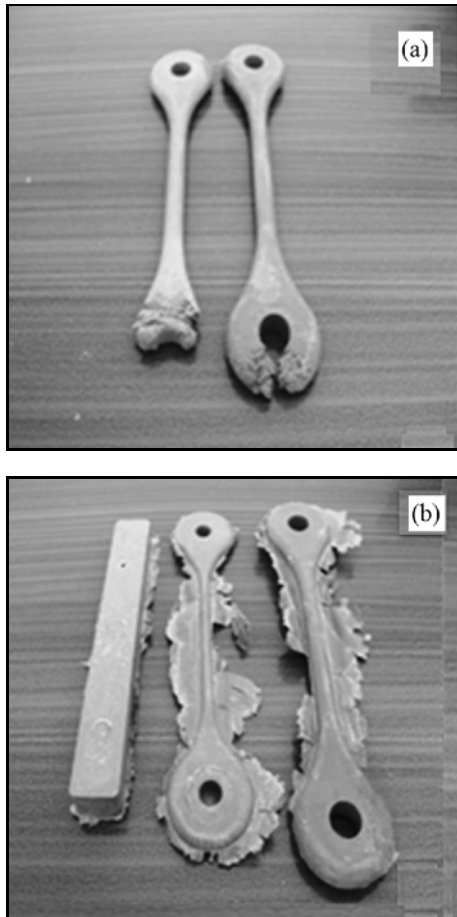


Fig. 12. Some defects of specimens: (a) incomplete filling and (b) ocular discharge.

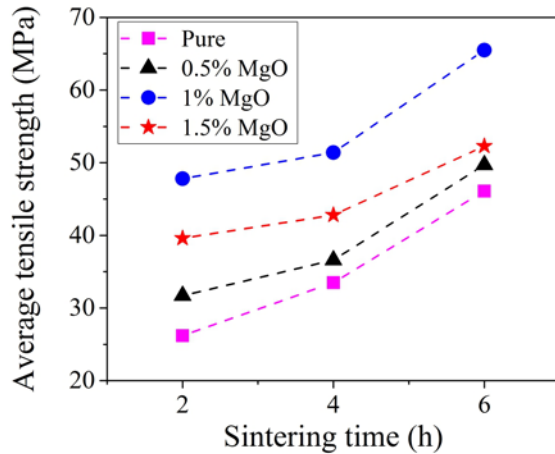
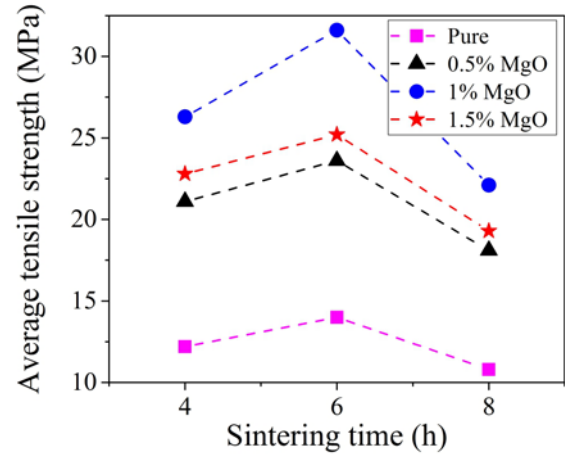
(Fig. 12a). After evaluating results, the pressure value was increased to 150 MPa and above, but this time, ocular discharge was observed on specimens (Fig. 12b). When it comes to the molding of bending specimens, 58.7 MPa pressure value was tested as a pre-operation parameter. However, the incomplete filling was ob-

served at this value similar to tensile specimens. Once the pressure was increased to 100 MPa, unfortunately, ocular discharge was again observed on specimens. As a result of unsuitable input parameters, incomplete filling, ocular discharge and collapses were observed in some molded samples depending on pressure, temperature, flow rate and the amount of getting feedstock. All in all, pre-operation parameter values obtained from Moldflow analysis results are useful regarding time and cost, but they are not sufficient for perfect specimen production. To avoid the experimental problems during the molding cycle, PIM operation parameters have been determined. Firstly, the cylinder temperature was kept constant within a certain range, and the pressure was increased in echelon. In this way, the most suitable molding pressure was determined. Afterwards, the pressure was held constant, and the other parameters (flow rate, temperature and the amount of getting feedstock) were changed one by one. Many trials were performed to produce standard and defect free specimens in PIM. Since the defects directly affect the quality of the final products, the most suitable PIM operation parameters have been determined (Table 5).

Pre-operation parameters (Table 4) were found to be lower than the actual molding parameters (Table 5). Although the rheological properties and physical properties of feedstocks were completely defined in the model, it was very normal that these differences occurred. The reason for this situation is that the solid alumina and MgO powder in the feedstock adversely affected the actual flow behavior of the feedstock. That is, the friction behavior between the feedstock and the mold surfaces, the behavior of the feedstock against the pressure, the ambient conditions and the working accuracy of the machine cannot be exactly simulated by the analysis program. Considering these reasons, it is inevitable that feedstocks containing powder additives are more resistant to flow. Therefore, in this study, the PIM operation param-

Table 6. The comparison of MPP and POP values and error amount (%)

	Molding pressure (MPa)			Feedstock flow rate ($\text{cm}^3 \text{s}^{-1}$)			Feedstock temperature ($^{\circ}\text{C}$)		
	MPP	POP	% error	MPP	POP	% error	MPP	POP	% error
Tensile	81.9	115	-28.7	13.8	17	-18.8	200	215	-7
Bending	58.7	95	-38.2	12.8	17	-24.7	200	215	-7

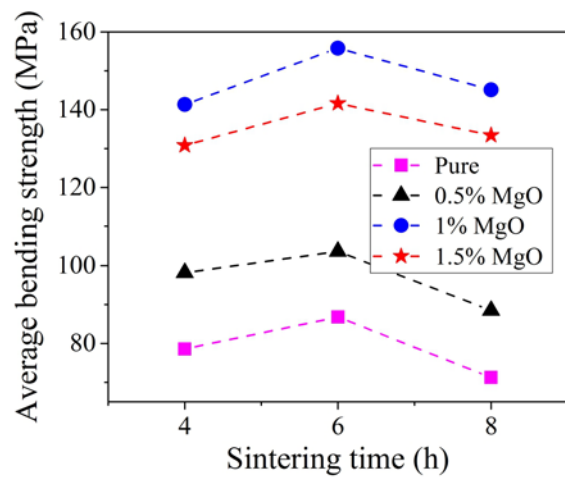
Fig. 13. The average tensile strength values of the small size tensile specimens sintered at 1775°C for 2, 4 and 6 h.Fig. 14. The average tensile strength values of the large size tensile specimens sintered at 1775°C for 4, 6 and 8 h.

eters (POP) obtained for the feedstocks have been determined at higher values than the Moldflow pre-operation parameters (MPP). As can be seen in Table 6, MPP and POP are compared, and % error rates are indicated. Since the MPP values are smaller than the POP values, the % error rates are expressed with a minus sign.

3.4. Debinding

In the solvent debinding tests, the best result was obtained after a 24-hour waiting time in the water at 60°C . After solvent debinding process, the specimens were dried at 50°C for 5 h in a furnace. The amount of PEG removed in water was 89 and 84 wt.% for the bending and the tensile test specimens, respectively.

The thermal debinding was carried out in the furnace at the beginning of the sintering process to remove the remaining binder components (PP and SA). Firstly, the specimens were heated at a rate of $3^{\circ}\text{C min}^{-1}$ up to 210°C and held for 30 min at this temperature. Secondly, the specimens were heated at a rate of $4^{\circ}\text{C min}^{-1}$ up to 480°C and held for 30 min at this temperature in the furnace. Lastly, they were heated at a rate of $5^{\circ}\text{C min}^{-1}$ up to 600°C and held for 15 min at this temperature. After successful removal of the binder, the specimens were kept in the furnace for sintering process.

Fig. 15. The average bending strength values of the bending specimens sintered at 1775°C .

3.5. Sintering and mechanical tests

The specimens were put into the furnace by placing them on ceramic plates. The ceramic plates were preferred to prevent adhesion of the specimens to the furnace surface at elevated temperatures. After the thermal debinding process, the furnace was reached to 600°C . The specimens were heated up to

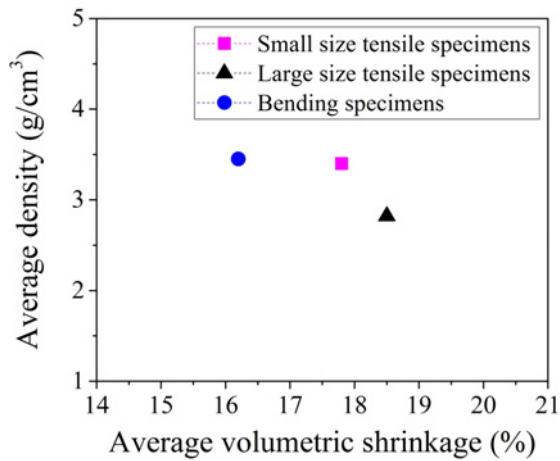


Fig. 16. The variation of average density vs. average volumetric shrinkage of specimens containing 1 wt.% MgO at sintered 1775°C for 6 h.

1200°C with 10°C min⁻¹ rate and held for 15 min at this temperature. To determine the most suit-

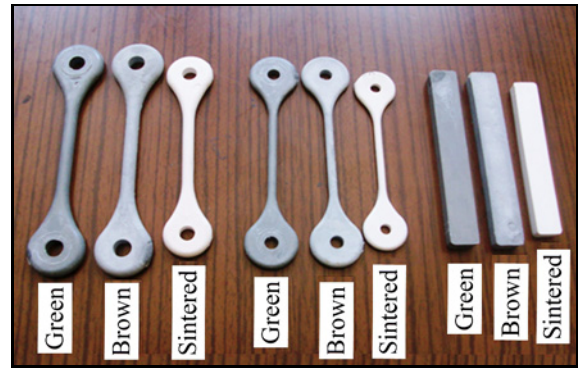


Fig. 17. Volumetric shrinkage of the specimens.

able sintering parameters, different specimens were heated up to 1650-1700-1720-1740-1750-1775-1790°C with 15°C min⁻¹ rate and held for 2–14 h in the furnace.

The first goal of the sintering experiments was to find the most suitable sintering temperature for the specimens. The specimens were deformed significantly

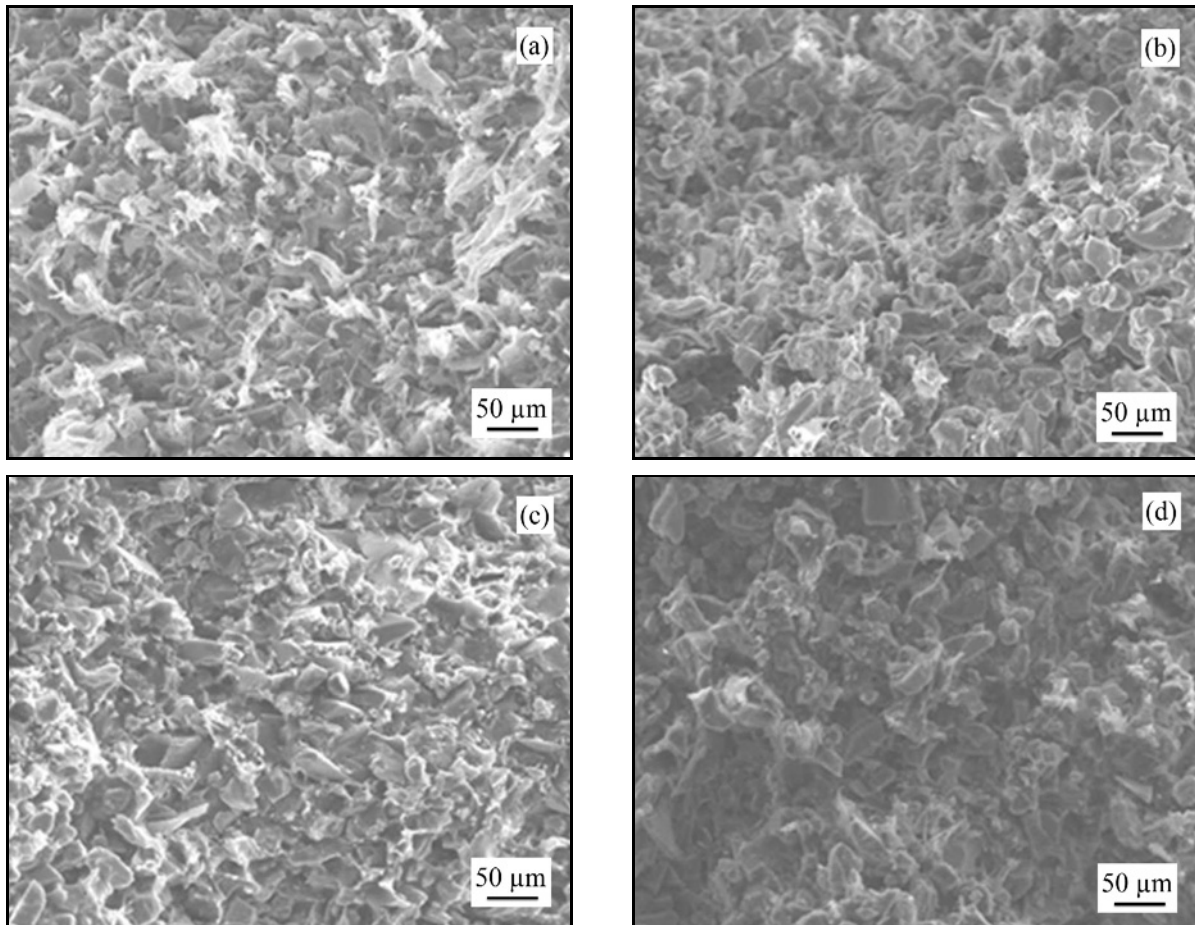


Fig. 18. The SEM images of green and brown specimens (pure): (a) green tensile specimen, (b) brown tensile specimen, (c) green bending specimen, and (d) brown bending specimen.

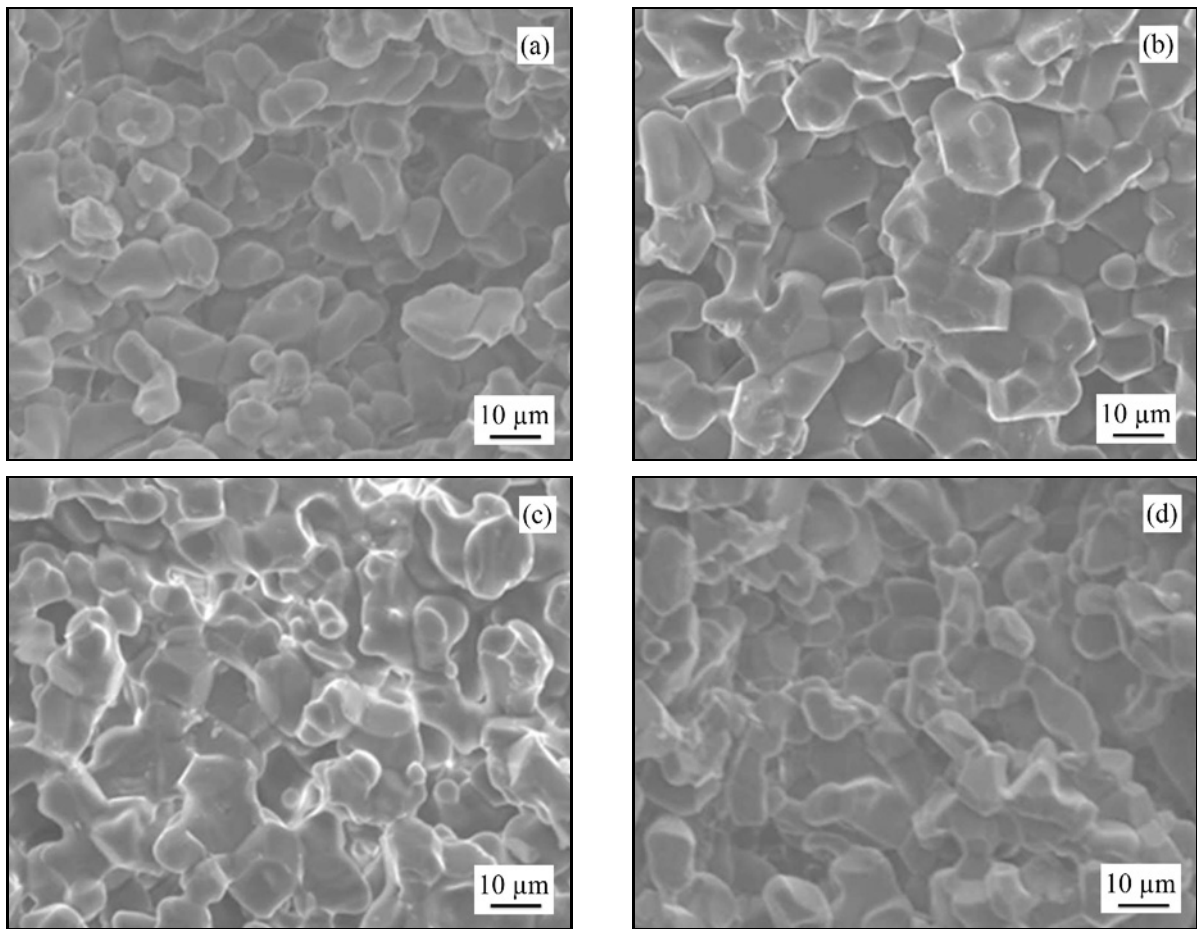


Fig. 19. The SEM images of tensile specimens' fractured surface with formulation of F2: (a) pure specimens; 48 MPa, (b) specimen containing 0.5 wt.% MgO; 50.4 MPa, (c) specimen containing 1 wt.% MgO; 69 MPa, and (d) specimen containing 1.5 wt.% MgO; 54.2 MPa.

at 1790 °C after waiting for 2 h (unsuitable for tensile tests). It has been decided that staying at this length of time, at this high temperature is also dangerous for the furnace. It was observed that the specimens sintered at 1775 °C for 2 h showed better strength properties than the specimens sintered at 1720 °C for 14 h. In sintering mechanism of alumina, the sintering temperature is more dominant than the holding time. So, waiting for a short while at high temperatures instead of waiting for longer time at low temperatures is preferable both for economic considerations and mass production suitability. As a result, the most suitable temperature was determined as 1775 °C. The second goal of the sintering experiments was to find the most suitable holding time for the specimens. The specimens were tested for 2, 4, 6, 8 and 10 h at 1775 °C. The small size tensile specimens sintered at 1775 °C for 8 and 10 h were significantly distorted. It was also observed that the large size tensile and bending specimens sintered at 1775 °C for 8 h had inferior mechanical properties. Consequently, 1775 °C temperature and 6 h holding time were determined as the most suitable sintering parameters.

Three specimens selected from each feedstock were subjected to the sintering process. The average tensile strength values of the tensile specimens sintered at 1775 °C for 2, 4, 6 and 8 h are shown in Figs. 13 and 14. The average bending strength values of the bending specimens sintered at 1775 °C for 4, 6 and 8 h are illustrated in Fig. 15. In Figs. 14 and 15, the reason for the strength reduction can be explained by the abnormal grain growth (AGG) in alumina during sintering. It has been accepted that AGG formation cannot be suppressed at the holding time (8 h) and so, mechanical properties are decreased due to this reason. This reasoning was also reported in the study of Park et al. [25] on abnormal grain growth in alumina with anorthite liquid and the effect of MgO addition. They stated that to increase density and strength of alumina, AGG must suppress and transform to normal grain growth behavior.

The addition of 0.5 wt.% MgO increased the tensile strength of all specimens. The specimens containing 1 wt.% MgO have the best strength values among the others. However, the addition of 1.5 wt.% MgO decreased the strength of all specimens. Moreover, the

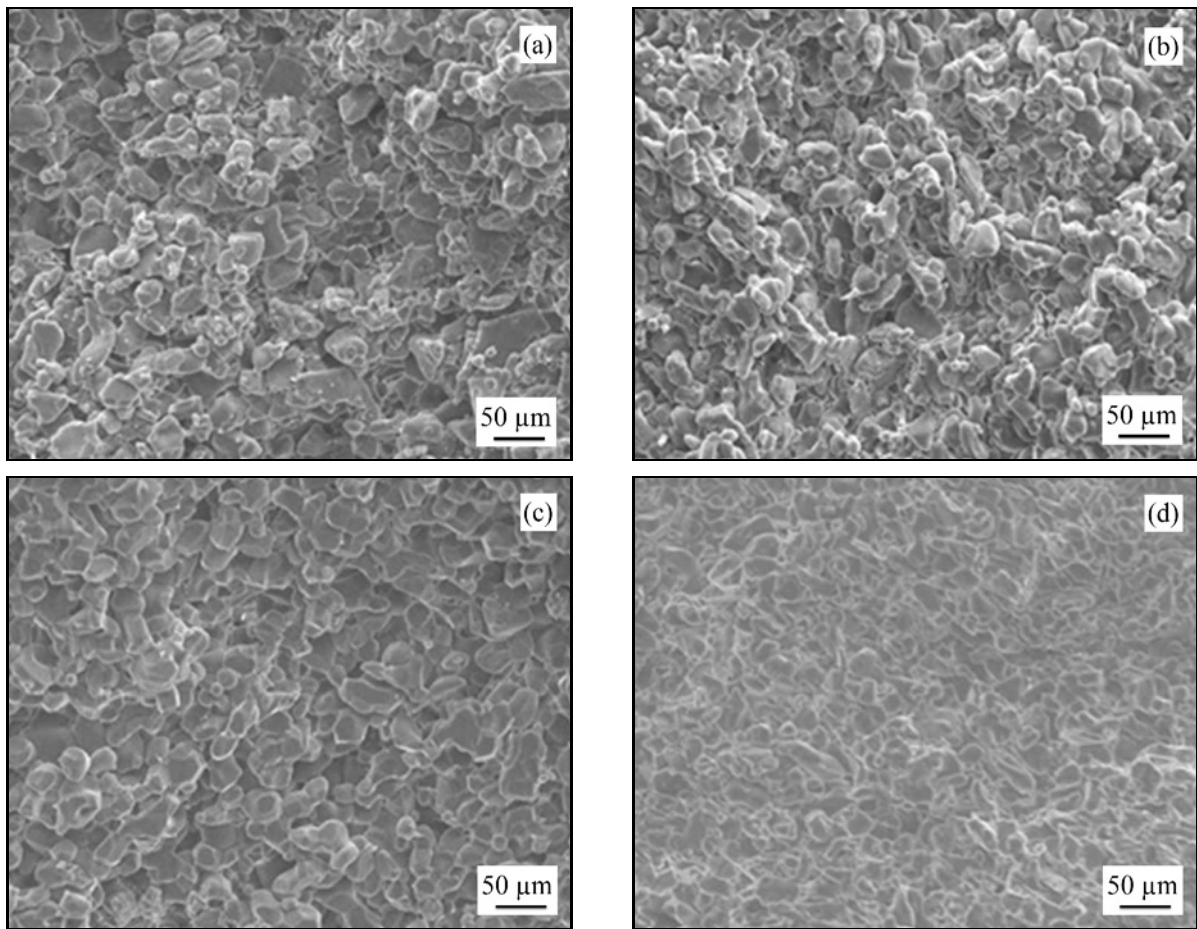


Fig. 20. The SEM images of bending specimens' fractured surface with formulation of F2: (a) pure specimens; 88.2 MPa, (b) specimen containing 0.5 wt.% MgO; 110 MPa, (c) specimen containing 1 wt.% MgO; 158 MPa, and (d) specimen containing 1.5 wt.% MgO; 144.1 MPa.

specimens sintered at 1775 °C for 8 h had inferior mechanical properties (Figs. 13–15).

3.6. Physical properties of sintered samples

The addition of MgO to alumina has shown the similar effects on density values as the strength values. Addition of 0.5 wt.% MgO increased the density of all specimens. It was obtained that specimens containing 1 wt.% MgO had the highest density values. However, the addition of 1.5 wt.% MgO decreased the density for all specimens. In Fig. 16, the variation of density vs. the average volumetric shrinkage of specimens containing 1 wt.% MgO is presented. Photographs of the green, brown (without binder) and sintered specimens are shown in Fig. 17. The sintered specimens are smaller than the others because they were densified and shrunk as pores almost disappeared at the end of the sintering.

SEM analysis was performed on the fractured surfaces of the specimens. The SEM images of the green and brown specimens are presented in Fig. 18. As can be seen in Figs. 18a and 18c, the green speci-

men binders (white color regions) are denser. As seen from Figs. 18b and 18d, the white color regions are decreased greatly in brown specimens. Typical SEM images of the specimens (tensile and bending) sintered at 1775 °C for 6 h are illustrated in Figs. 19 and 20. As can be seen in Figs. 19c and 20c, the specimens (tensile and bending) containing 1 wt.% MgO have less porosity (i.e., these specimens are denser than the others).

4. Conclusions

The influence of MgO addition to the mechanical properties of the injection molded alumina was investigated. On the view of our experiments, we may conclude the following:

1. Different feedstocks (F1, F2, F3 and F4) were examined under 18.7 kPa shear stress value at 170–210 °C temperatures. F2 showed the most proper pseudo-plastic behavior. So, the optimum powder/binder ratio was chosen as 53/47 vol.% (F2).

2. Although Moldflow pre-operation parameter (MPP) values have been useful regarding time and

cost, they have not been sufficient for perfect specimen production. So, many trials were performed to produce standard and defect free specimens. When the experimental study was compared with the analysis study, the error rates of -28.7% on the tensile specimen and -38.2% on the bending specimen were determined for the injection pressure value. The error rate of flow rate was -18.8% for the tensile specimen and -24.7% for the bending specimen. An error rate of -7% was determined for both the tensile and bending specimens for the feedstock temperature.

3. In the solvent debinding tests, the best result was obtained after a 24-hour waiting time in the water at 60°C . The amount of PEG removed in the water was 89 wt.% and 84 wt.% for the bending and tensile test specimens, respectively.

4. The specimens sintered at 1775°C for 8 h had inferior mechanical properties. The reason for the strength reduction can be explained as the AGG in alumina during sintering. It has been accepted that AGG formation cannot be suppressed at the holding time (8 h).

5. The addition of 0.5 wt.% MgO increased the strength of all specimens. The specimens containing 1 wt.% MgO had the best strength values among the others. However, the addition of 1.5 wt.% MgO decreased the strength of all specimens. The maximum strengths of bending and tensile test values were found 158 and 69 MPa (in specimens containing 1 wt.% MgO), respectively.

6. The addition of MgO to alumina had shown the similar effects on density values like the strength values. The maximum density of bending and tensile test values were found 3.49 g cm^{-3} and 3.44 g cm^{-3} (in specimens containing 1 wt.% MgO), respectively.

Acknowledgements

The authors acknowledge the support of Gazi University (BAP Project No: 06/2010-14) and the Dumlupinar University (BAP Project No: DPU BAP 2013-2) for facilitating the experimental and simulation studies.

References

- [1] Bleyan, D., Hausnerova, B., Svoboda, P.: Powder Technol., 286, 2015, p. 84. [doi:10.1016/j.powtec.2015.07.046](https://doi.org/10.1016/j.powtec.2015.07.046)
- [2] German, R. M.: Powder Injection Molding. New York, Princeton 1990.
- [3] Kong, X., Barriere, T., Gelin J. C.: J. Mater. Process. Technol., 212, 2012, p. 2173. [doi:10.1016/j.imatprotec.2012.05.023](https://doi.org/10.1016/j.imatprotec.2012.05.023)
- [4] Kate, K. H., Enneti, R. K., McCabe, T., Sundar Atre, S. V.: Ceramics International, 42, 2016, p. 194. [doi:10.1016/j.ceramint.2015.08.079](https://doi.org/10.1016/j.ceramint.2015.08.079)
- [5] Meng, J., Loh, N. H., Fu, G., Tay, B. Y., Tor, S. B.: J. Eur. Ceram. Soc., 31, 2011, p. 1049. [doi:10.1016/j.jeurceramsoc.2010.11.034](https://doi.org/10.1016/j.jeurceramsoc.2010.11.034)
- [6] Lu, Z., Zhang, K., Wang, C.: Powder Technol., 208, 2011, p. 49. [doi:10.1016/j.powtec.2010.12.002](https://doi.org/10.1016/j.powtec.2010.12.002)
- [7] Murakami, S., Ri, K., Itoh, T., Izu, N., Shin, W., Inukai, K., Takahashi, Y., Ando Y.: Ceramics International, 38, 2012, p. 1591. [doi:10.1016/j.ceramint.2011.09.046](https://doi.org/10.1016/j.ceramint.2011.09.046)
- [8] Nuruzzaman, D. M., Kusaseh, N., Basri, S., Oumer, A. N., Hamedon, Z.: Materials Science and Engineering, 114, 2016, p. 1. [doi:10.1088/1757-899X/114/1/012043](https://doi.org/10.1088/1757-899X/114/1/012043)
- [9] Wanga, X., Zhao, G., Wanga, G.: Materials and Design, 47, 2013, p. 779. [doi:10.1016/j.matdes.2012.12.047](https://doi.org/10.1016/j.matdes.2012.12.047)
- [10] Rahman, W. A., Sin, L. T.: J. Mater. Process. Technol., 197, 2008, p. 22. [doi:10.1016/j.jmatprotec.2007.06.014](https://doi.org/10.1016/j.jmatprotec.2007.06.014)
- [11] Liu, W., Xie, Z., Jia, C.: J. Eur. Ceram. Soc., 32, 2012, p. 1001. [doi:10.1016/j.jeurceramsoc.2011.11.017](https://doi.org/10.1016/j.jeurceramsoc.2011.11.017)
- [12] Gelin, J. C., Barriere, Th., Song, J.: ASME J. Eng. Mater. and Technol., 132, 2010, p. 1. [doi:10.1115/1.2931155](https://doi.org/10.1115/1.2931155)
- [13] Krauss, V. A., Oliveira, A. A. M., Klein, A. N., Al-Qureshi, H. A., Fredel, M. C.: J. Mater. Process. Technol., 182, 2007, p. 268. [doi:10.1016/j.jmatprotec.2006.08.004](https://doi.org/10.1016/j.jmatprotec.2006.08.004)
- [14] Mannschatz, A., Höhn, S., Moritz, T.: J. Eur. Ceram. Soc., 30, 2010, p. 2827. [doi:10.1016/j.jeurceramsoc.2010.02.020](https://doi.org/10.1016/j.jeurceramsoc.2010.02.020)
- [15] Oliveira, R. V. B., Soldi, V., Fredel, M. C., Pires, A. T. N.: J. Mater. Process. Technol., 160, 2005, p. 213. [doi:10.1016/j.jmatprotec.2004.06.008](https://doi.org/10.1016/j.jmatprotec.2004.06.008)
- [16] He, Z., Ma, J.: Computational Materials Science, 32, 2005, p. 196. [doi:10.1016/j.commatsci.2004.08.006](https://doi.org/10.1016/j.commatsci.2004.08.006)
- [17] Loebbecke, B., Knitter, R., Haußelt, J.: J. Eur. Ceram. Soc., 29, 2009, p. 1595. [doi:10.1016/j.jeurceramsoc.2008.11.001](https://doi.org/10.1016/j.jeurceramsoc.2008.11.001)
- [18] Toniolo, J. C., Lima, M. D., Takimi, A. S., Bergmann, C. P.: Materials Research Bulletin, 40, 2005, p. 561. [doi:10.1016/j.materresbull.2004.07.019](https://doi.org/10.1016/j.materresbull.2004.07.019)
- [19] Junchang, L., Bolin, W.: Journal of Alloys and Compounds, 695, 2017, p. 2324. [doi:10.1016/j.jallcom.2016.11.099](https://doi.org/10.1016/j.jallcom.2016.11.099)
- [20] Roh, J. Y., Kwon, J., Lee, C. S., Choi, J. S.: Ceramics International, 37, 2011, p. 321. [doi:10.1016/j.ceramint.2010.09.011](https://doi.org/10.1016/j.ceramint.2010.09.011)
- [21] Liu, C., Sun, J., Xie, Z.: Journal of Alloys and Compounds, 546, 2013, p. 102. [doi:10.1016/j.jallcom.2012.08.097](https://doi.org/10.1016/j.jallcom.2012.08.097)
- [22] Sathiyakumar, M., Gnanam, F. D.: J. Mater. Process. Technology, 133, 2003, p. 282. [doi:10.1016/S0924-0136\(02\)00956-1](https://doi.org/10.1016/S0924-0136(02)00956-1)
- [23] Hwang, K. S., Hsieh, C. C.: J. Am. Ceram. Soc., 88, 2005, p. 2349. [doi:10.1111/j.1551-2916.2005.00370.x](https://doi.org/10.1111/j.1551-2916.2005.00370.x)
- [24] Gavrilov, K. L., Bennison, S. J., Mikeska, K. R., Levi-Setti, R.: J. Mater. Sci., 38, 2003, p. 3965. [doi:10.1023/A:1026206414377](https://doi.org/10.1023/A:1026206414377)
- [25] Park, C. W., Yoon, D. Y.: J. Am. Ceram. Soc., 85, 2002, p. 1585. [doi:10.1111/j.1151-2916.2002.tb00316.x](https://doi.org/10.1111/j.1151-2916.2002.tb00316.x)
- [26] Heraiz, M., Merrouche, A., Saheb, N.: Advances in Applied Ceramics, 105, 2006, p. 285.

- [doi:10.1179/174367606X146676](https://doi.org/10.1179/174367606X146676)
- [27] Mannschatz, A., Müller, A., Moritz, T.: *J. Eur. Ceram. Soc.*, 31, 2011, p. 2551.
[doi:10.1016/j.jeurceramsoc.2011.01.013](https://doi.org/10.1016/j.jeurceramsoc.2011.01.013)
- [28] Liu, W., Xie, Z., Bo, T., Yang, X.: *J. Eur. Ceram. Soc.*, 31, 2011, p. 1611.
[doi:10.1016/j.jeurceramsoc.2011.03.003](https://doi.org/10.1016/j.jeurceramsoc.2011.03.003)
- [29] Karatas, C., Kocer, A., Ünal, H. I., Saritas, S.: *J. Mater. Process. Technol.*, 152, 2004, p. 77.
[doi:10.1016/j.jimatprotec.2004.03.009](https://doi.org/10.1016/j.jimatprotec.2004.03.009)
- [30] Sidambe, A. T., Figueroa, I. A., Hamilton, H., Todd, I.: *Mater. Sci. Eng.*, 26, 2011, p. 1.
[doi:10.1088/1757-899X/26/1/012005](https://doi.org/10.1088/1757-899X/26/1/012005)
- [31] Urtekin, L., Uslan I., Tuc, B.: *J. Mater. Eng. and Perf.*, 21, 2012, p. 358. [doi:10.1007/s11665-011-9901-8](https://doi.org/10.1007/s11665-011-9901-8)